

Notes to the Editor

Annealing and melting behaviour of poly(1-butene), modification I

J. Haase, R. Hosemann and S. Köhler

Fritz-Haber-Institut der MPG, Teilinstitut für Strukturforschung, Berlin-Dahlem, West Germany
(Received 20 April 1978)

INTRODUCTION

Combined wide-angle X-ray scattering (WAXS) and differential thermal analysis (d.t.a.) on isotactic poly(1-butene), modification I (Mod. I) gives a new insight into the melting behaviour of polymers and leads to a different interpretation from conventional theories.

EXPERIMENTAL

Samples of poly(1-butene) were melted at 180°C and quenched to room temperature. On quenching the metastable modification II (Mod. II) crystallizes, and then slowly transforms into the stable Mod. I. By this transformation, the crystallinity remains constant¹ and the crystallite sizes change by 10–15%, because the lattice constant, c , and the density increase by about 15 and 7%, respectively. The half-life of Mod. II in a quenched sample is of the order of 10³ min at room temperature and infinitely large at temperatures above 100°C. On subsequent annealing immediately after quenching i.e. on annealing in Mod. II at different temperatures for different times, samples with a wide variety of crystallite sizes were obtained. Special interest was focussed on two samples near the extremes of the crystallite size spectrum: sample A, quenched; and sample B, quenched and subsequently annealed (in Mod. II) for 10³ min at 110°C and then quenched again. All WAXS and d.t.a. measurements were performed after transformation of Mod. II into Mod. I.

CRYSTALLITE SIZE DISTRIBUTIONS AND D.T.A. CURVES

In Figure 1 peak melting points, T_m , are plotted versus the reciprocal of the mean crystallite size, \bar{D}_{012} , which is an

excellent approximation for the size in chain direction². The linear relationship may be explained by the well known 'Thomson equation'³:

$$T_m = T_m^\infty \left(1 - \frac{2\sigma_e'}{\Delta h_f \bar{D}_{012}} \right) \quad (1)$$

with a melting point of $T_m^\infty = 138.6^\circ\text{C}$ for an infinite crystal and a surface free energy of $\sigma_e' = 47 \text{ erg/cm}^2$ assuming the heat of fusion per unit volume of an infinite crystal $\Delta h_f = 1675 \text{ cal/monomer unit}^4$ and its density $\rho_c = 0.95 \text{ g/cm}^3$.

Equation (1) is derived from the melting point formula for a chain-folded crystal, of length l and lateral dimensions a and b having a fold surface free energy σ_e and a lateral surface free energy σ , as follows:

$$T_m = T_m^\infty \left(1 - \frac{2\sigma_e}{\Delta h_f l} - \frac{2\sigma}{\Delta h_f a} - \frac{2\sigma}{\Delta h_f b} \right) \quad (2)$$

This formula can be expanded further by a term describing the melting point depression by lattice distortions⁵. If $\sigma_e \gg \sigma$, and or $a, b \gg l$, then equation (1) is valid with:

$$\bar{\sigma}_e' = \sigma_e \quad (\text{and } \bar{D}_{012} = l)$$

Otherwise σ_e is smaller than $\bar{\sigma}_e'$, i.e. the lateral surface free energy contributes to the melting point depression.

From the measured 012 wide-angle line profiles we obtained the crystallite size mass distributions in the chain direction, defined by the polydispersity g_D ⁶.

$$g_D = (\bar{D}^2/\bar{D}^2 - 1)^{1/2} \quad (3)$$

Giving each crystallite size a melting point according to the Thomson equation, a theoretical d.t.a. curve can be calculated from the size distribution.

These theoretical d.t.a. curves for samples A and B are compared with the experimental ones (full lines) in Figure 2. The corresponding widths δT of the d.t.a. curves, taken at half peak height, are seen from Table 1.

There is undoubtedly no agreement. The experimental d.t.a. curve may be broader (see A in Figure 2) or sharper (see B in Figure 2) than the theoretical one. Therefore, the equation (1) with a constant surface free energy σ_e' for the different crystallite sizes in the same sample cannot explain the experimental d.t.a. curves. This will be strongly supported by the facts dealt with below. From the excellent linear relationship between melting point and mean crystallite size in chain direction (see Figure 1), it must be concluded that σ_e' is the same for all these samples.

Table 1 Experimental and calculated widths δT of d.t.a. curves, taken at half peak height, for different samples of poly(1-butene), modification I (see Figures 1 and 2)

Sample	$\delta T_{\text{exp}} (^\circ\text{C})$	$\delta T_{\text{calc}} (^\circ\text{C})$
A	11.1	6.5
B	2.2	5.4
A [*]	1.5	4.5
B [*]	(<1.0)	1.8

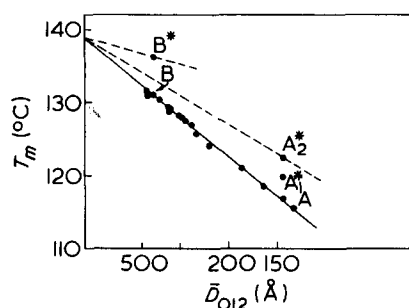


Figure 1 Peak melting points of poly(1-butene) samples in modification I versus the reciprocal mean crystallite size in chain direction; line A–B; samples annealed in modification II; A^{*}, A₂^{*}, B^{*}, samples annealed in modification I (see text and Table 3)

Table 2 Mean crystallite size in chain direction, \bar{D}_{012} , the polydispersity of the crystallite size mass distribution in this direction, g_D , the mean crystallite size in a lateral direction, \bar{D}_{110} , and the paracrystalline g_{110} value during melting of poly(1-butene), modification I, sample B

T (°C)	Mod. I (% molten)	\bar{D}_{012} (Å)	g_D (012)	\bar{D}_{110} (Å)	g_{110} (%)
125.0	0	426	0.37	640	1.8
131.0	41	420	0.37	780	2.2
132.0	63	422	0.38	660	1.8
132.5	78	429	(0.40)	680	2.1
133.0	88	(410)		710	2.0

Table 3 Melting point T_m , d.t.a. crystallinity α , mean surface free energy $\bar{\sigma}'_e$ and some WAXS results (see *Table 2*) for poly(1-butene), modification I, sample A annealed at 113°C for different times t_{ann}

Sample	t_{ann} (h)	T_m (°C)	\bar{D}_{012} (Å)	g_D (012)	\bar{D}_{110} (Å)	g_{110} (%)	α (%)	$\bar{\sigma}'_e$ (erg/cm ²)
A	0	116.8	146	0.16	378	1.9	36	47
A ₀ *	1	117.9	—	—	421	1.7	—	44
A ₁ *	10	119.8	—	—	—	—	—	40
A ₂ *	100	122.6	148	0.16	415	1.7	35	34

ANNEALING AND MELTING BEHAVIOUR

Crystal characteristics

Mean crystallite sizes \bar{D} , polydispersities g_D and lattice distortions — the amount of which is characterized by the paracrystalline g value — have been measured successively at different temperatures, T . In *Table 2* the results for sample B are plotted as a function of the molten percent of Mod. I, calculated from the integral reflection intensities.

The results for sample A are similar. They show that there are no changes in mean crystallite sizes, the crystallite size distributions, or the lattice distortions during annealing and melting. We may, therefore, conclude:

(i) Melting of poly(1-butene), Mod. I, is not at all selective regarding the different crystallite sizes only⁷. If it were so, the mean crystallite size in the chain direction should increase and its polydispersity should decrease during melting.

(ii) Melting of poly(1-butene), Mod. I, is not in agreement with the surface premelting model⁸. This model predicts that either the crystallite size in the chain direction should decrease (the lateral size being constant) or the lateral crystallite size should decrease (the crystallite size in the chain direction being constant) during melting.

(iii) Considering the lattice distortions within the crystallites measured by the paracrystalline g_{110} value, melting of poly(1-butene), Mod. I, does not proceed in such a way that the less perfect crystals melt first⁵.

Annealing

Other striking results are obtained when sample A is annealed at 113°C for 1 h (sample A₀*), 10 h (sample A₁*), and 100 h (sample A₂*) (see *Table 3* and *Figures 1* and 2). Although the crystallites of poly(1-butene), Mod. I, do not thicken and the crystallite size distribution in the chain direction does not change on annealing, the peak melting point increases and the width of the d.t.a. curve decreases drastically.

According to equation (1), the increase of T_m with annealing time, which is a slow process (see *Table 3*), must be associated with a decrease of the mean surface free energy $\bar{\sigma}'_e$ (see last column in *Table 3*). By successive annealing of sample B at different and increasing temperatures, we could finally shift its melting point to $T_m = 136.2^\circ\text{C}$, corresponding to a mean surface free energy of only $\bar{\sigma}'_e = 15$ erg/cm² (sample B* in *Figures 1* and 2). Similar results have been published recently for isotactic polystyrene⁹.

Part of the decrease of the d.t.a. width δT on annealing must be attributed to this decrease of $\bar{\sigma}'_e$, as is shown by the comparison of the theoretical curves (broken lines) of samples A and A₂* in *Figure 2*, which are calculated from the same crystallite size mass distribution and $\bar{\sigma}'_e = 47$ and 34 erg/cm², respectively. In addition, however, there must be a narrowing of the (σ'_e/D_{012}) distribution on annealing.

The question arises, where does the melting process in the sample start, i.e. where are the high (σ'_e/D) values located? As the unprotected surfaces have

a higher surface free energy, we conclude that melting starts preferentially at locations where lamellae end^{10,11}, thus creating unprotected lateral and unprotected fold surfaces.

SUMMARY

(1) Lamellar crystals of isotactic poly(1-butene), modification I, with mean thicknesses between 140 and 460 Å do not thicken on annealing at temperatures up to the melting point, though more and more material is transferred to the molten state.

(2) As shown by WAXS, not only the mean size in chain direction \bar{D}_{012} of the microparacrystallites, but also the polydispersity of the crystallite size mass distribution in this direction, the mean size in a lateral direction, \bar{D}_{110} , and the paracrystalline lattice distortions do not change if measured at elevated temperatures up to the melting point. This proves that neither surface premelting nor selective melting of thinner or more distorted microparacrystallites takes place.

(3) The shape of the d.t.a. curve, therefore, gives no information on the size distribution of the microparacrystallites. It can be broader or sharper than that calculated from the Thomson equation by means of the crystallite size mass distribution in the chain direction.

(4) The surface free energy $\bar{\sigma}'_e$, therefore, is not a constant for the different crystallite sizes in one and the same sample. The Thomson equation applied to different samples, on the other hand, links only the average crystallite size and the mean surface free energy $\bar{\sigma}'_e$ with the melting point.

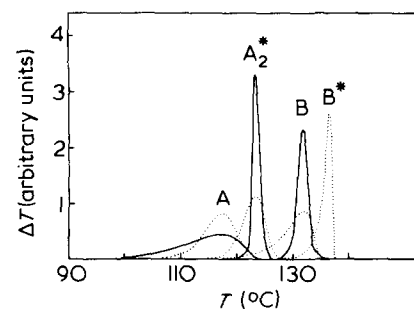


Figure 2 D.t.a. curves of different samples of poly(1-butene), modification I (see *Figure 1*): —, experimental curves; - - -, theoretical curves calculated from the crystallite size mass distribution by means of the Thomson equation. The experimental curves of samples A₂* and B* are refolded by the d.t.a. instrument profile. The refolded curve of sample B* was omitted, because of its great error; its width, δT , should be smaller than 1°C (see *Table 1*)

(5) Although crystallite sizes, size distributions and paracrystalline lattice distortions remain constant, the d.t.a. curve shifts to higher temperatures and becomes sharper on annealing. This can be explained only by assuming that the average surface free energy $\bar{\sigma}_e$ decreases and that the distribution of the (σ'_e/D_{012}) values narrows on annealing.

(6) The melting process starts preferentially at locations, where lamellae end, thus creating unprotected lateral and fold surfaces with high σ'_e values. This confirms the published¹¹ mechanism of increasing long period and

lamellae thickness during annealing and heating.

ACKNOWLEDGEMENTS

Thanks are due to Dr G. Goldbach (Chemische Werke Hüls) for supplying the samples of poly(1-butene).

REFERENCES

- 1 Rubin, I. R. *J. Polym. Sci. (B)* 1964, **2**, 747
- 2 Haase, J., Hosemann, R. and Renwanz, B. *Colloid Polym. Sci.* 1977, **255**, 849
- 3 Hoffman, J. D. in 'Treatise on Solid

State Chemistry', Plenum Press, 1976, Vol 3

- 4 Wilski, H. and Grever, T. *J. Polym. Sci. (C)* 1964, **6**, 33
- 5 Sanchez, I. R. and Eby, R. K. *J. Res. Nat. Bur. Stand. (A)* 1973, **77**, 774
- 6 Hosemann, R. and Bagchi, S. N. in 'Direct Analysis of Diffraction by Matter' North-Holland, Amsterdam, 1962
- 7 Kilian, H. G. *Kolloid Z. Z. Polym.* 1969, **231**, 534
- 8 Fischer, E. W. *Kolloid Z. Z. Polym.* 1969, **231**, 458
- 9 Overbergh, N., Berghmans, H. and Reynaers, H. *J. Polym. Sci.* 1976, **14**, 1177
- 10 Petermann, J., Miles, M. and Gleiter, H. *J. Macromol. Sci. (B)* 1976, **12**, 393
- 11 Hosemann, R. *Polymer* 1962, **3**, 349

An improved graphical method for the evaluation of molecular weight measurements on polymers

T. T. Nagy, T. Kelen and F. Tüdös

Central Research Institute for Chemistry of the Hungarian Academy of Sciences, Budapest, Hungary

(Received 4 April 1978; revised 13 June 1978)

We have previously suggested a new linear graphical method with several advantages for the determination of copolymerization constants¹. By this method, the straight line:

$$y = ax + b \quad (1)$$

with introduction of the new variables

$$f = \frac{x}{\gamma + x} \quad \text{and} \quad g = \frac{y}{\gamma + x} \quad (2)$$

is transformed into the straight line

$$g = a'f + b' \quad (3)$$

by the application of which the parameters

$$a = a' + b' \quad \text{and} \quad b = b'\gamma \quad (4)$$

can be determined from the data points with better reliability than by the application of the original equation (1).

In the above relations, γ is an appropriately chosen constant. In copolymerization systems, the most feasible procedure proved to be²⁻⁵ to choose the γ value so as to obtain experimental points in the most extended and at the same time most symmetrical arrangement; then from the determining equation:

$$f_m = 1 - f_M \quad (5)$$

we have

$$\gamma = \sqrt{x_m x_M} \quad (6)$$

(where the lowest f and x values are denoted by f_m and x_m and the highest by f_M and x_M , respectively).

Our choice of the auxiliary parameter, γ may be governed, however, by other principles as well, e.g. by the requirement of obtaining a more uniform error distribution by the transformation, in order to increase the reliability of evaluation. This is possible if the standard deviation of measurement can be given in a simple form, e.g. as an explicit function of the independent variable.

In such a case, for the determining equation we have:

$$\sigma(g_m) = \sigma(g_M) \quad (7)$$

i.e. the γ value must be chosen so that the transformation yields identical standard deviations (σ) for data measured at the lowest and highest independent variables.

In this Note we deal with the specific, though not unique case when the standard deviation of the data is inversely proportional to the value of the independent variable. This is the case for osmometric and viscometric molecular weight determinations when (π/c) versus (η_{sp}/c) data are extrapolated to zero concentration. The standard deviations of the osmotic pressure

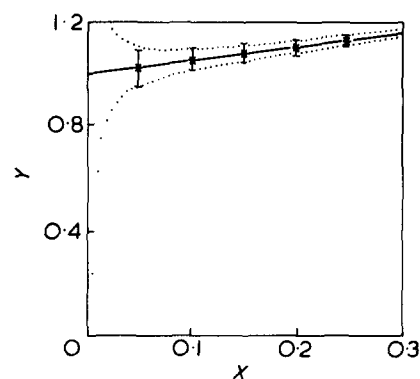


Figure 1 Measured $y = \eta_{sp}/c$ values as a function of $x = c$ concentration. The stars denote the average of 30 measurements. Broken lines are calculated scatter curves

$\sigma(\pi)$ and of the specific viscosity $\sigma(\eta_{sp})$ are nearly constant. Using the symbols $y = \pi/c$ vs. η_{sp}/c and $x = c$ as in equation (1), we have $\sigma(y) = \sigma(\pi)/x$ vs. $\sigma(\eta_{sp})/x$ and $\sigma(y)$ is inversely proportional to x : $\sigma(y) \approx 1/x$. According to this treatment:

$$\sigma(g) = \frac{\sigma(y)}{\gamma + x} \approx \frac{1/x}{\gamma + x} \quad (8)$$

in other words, the determining equation (7) of γ auxiliary parameter is then:

$$\frac{1/x_m}{\gamma + x_m} = \frac{1/x_M}{\gamma + x_M} \quad (9)$$